

**PIV/LDV MEASUREMENTS OF MEAN VELOCITY AND  
TURBULENCE IN A COMPLEX OPEN CHANNEL FLOW**

**By**

**B-S. Hyun, R. Balachandar, K. Yu, and V.C. Patel**



**IIHR Technical Report No. 424**

**IIHR—Hydroscience & Engineering  
College of Engineering  
The University of Iowa  
Iowa City, Iowa 52242-1585 USA**

**April 2003**

## TABLE OF CONTENTS

	<u>Page</u>
LIST OF FIGURES .....	ii
ABSTRACT.....	iii
INTRODUCTION .....	1
TEST CASE: OPEN CHANNEL FLOW OVER A BED OF FIXED DUNES.....	3
EXPERIMENTAL ARRANGEMENT AND PROCEDURE.....	4
RESULTS AND DISCUSSIONS.....	6
Instantaneous flow field.....	7
Time-averaged flow field.....	7
Time series data and two-point correlation.....	9
Quadrant analysis.....	10
FURTHER DISCUSSION ON THE ACCURACY OF PIV .....	11
Interrogation area and searching distance.....	11
Effect of time resolution .....	12
Effect of total number of data .....	12
Particle size and density .....	13
CONCLUSIONS.....	14
ACKNOWLEDGMENTS .....	14
REFERENCES .....	14

## LIST OF FIGURES

<u>Figure</u>		<u>Page</u>
1	Schematic of flow and notation .....	17
2	Experimental arrangement .....	17
3	Instantaneous velocity field obtained by PIV .....	18
4	Time-averaged flow field by PIV .....	19
5	Comparison between PIV and LDV data.....	20
6	Time series data from PIV .....	21
7	Two-point correlations at $X/h = 4$ , $Y/h = 0.53$ .....	22
8	Quadrant analysis at $X/h = 4$ , $x/\lambda = 0.2$ .....	22

## **PIV/LDV Measurements of Mean Velocity and Turbulence in a Complex Open Channel Flow**

B-S. Hyun, R. Balachandar, K. Yu, and V.C. Patel

### **ABSTRACT**

The complementary nature of PIV and LDV, in readily available configurations, is demonstrated along with their strengths and limitations in complex water flow fields. To this end, the flow over a fixed two-dimensional dune in an open channel is explored. This flow field is well suited to evaluate the relative performance of the two techniques and contains much of the complexity noted in practical hydraulic engineering applications. Agreement in the data obtained with the two techniques even in regions of flow reversals and high shear show that the PIV is fast reaching a stage where it can be applied with confidence in complex turbulent flows. It should be noted that this assessment is limited to measuring systems that are readily available or can be assembled by researchers who are not dedicated to the exclusive development of cutting-edge techniques.

# **PIV/LDV Measurements of Mean Velocity and Turbulence in a Complex Open Channel Flow**

B-S. Hyun<sup>1</sup>, R. Balachandar<sup>2</sup>, K. Yu<sup>3</sup> and V.C. Patel<sup>4</sup>  
IIHR – Hydrosience & Engineering<sup>5</sup>  
The University of Iowa  
Iowa City, IA 52242, USA

## **INTRODUCTION**

Laser Doppler velocimetry (LDV) and particle image velocimetry (PIV) are now recognized as well established non-intrusive techniques for fluid velocity measurement. Since the first use of LDV over almost four decades ago (Yeh and Cummins, 1964), several refinements have taken place making it the standard in velocity measurement, especially in water. LDV has now been used to make velocity measurements in a variety of complex flow fields and comprehensive descriptions of typical systems can be found in Goldstein (1996). Besides resolving a detailed temporal evolution of the flow field at the point of measurement, LDV provides information on the mean velocity, Reynolds stresses, and higher-order moments, such as skewness, flatness factor, and triple correlations, with a high degree of accuracy over a large dynamic range. Apart from the limitations connected to seeding of the flow, which are common to all optical techniques, LDV remains largely a single point measurement technique and does not provide information on the spatial structure of the flow, although simultaneous use of two or more systems can yield more information (Nezu et al., 1997).

Though PIV had its genesis several years ago, its more common usage has occurred in the last decade. The ability of PIV, in principle, to provide information over a flow field, simultaneously at many points, will ensure use to become even more widespread. The bibliography of Adrian (1996) gives an indication of the historical development of PIV, while different PIV techniques are described in Adrian (1991) and Raffel et al., (1998). Several recent studies (Cenedese et al., 1994; Nakagawa and

---

<sup>1</sup> Professor, Korea Maritime University, Pusan, Korea

<sup>2</sup> Professor & Head, University of Windsor, Windsor, Canada

<sup>3</sup> Graduate Research Assistant

<sup>4</sup> Professor and Director

<sup>5</sup> Formerly Iowa Institute of Hydraulic Research

Hanratty, 2001, Shineeb et al., 2002) have demonstrated the application of PIV to complex flows. An important aspect of PIV is its ability to measure the vorticity field and spatial correlations (Nezu and Onitsuka, 2001; Nezu and Nakayama, 1997). To some extent, PIV still suffers limitations in the dynamic range of velocity measurement though significant improvements have been made (Adrian 1997). Other limitations on the quality of data are placed by the size of seed particles, image quality and size, camera frame rate, processing software, etc.

In spite of the increasing use of both LDV and PIV, only a few researchers have used the two techniques jointly, and therefore, assessment of the relative merits of the two techniques is rather limited. For example, in studying rough wall boundary layers, Keirsbulck et al., (2002) conducted LDV and PIV measurements but their comparison between data obtained with the two systems was limited to a qualitative discussion. In other instances, the comparisons mainly dealt with evaluating the mean velocity profiles at representative cross-sections in the flow field. For example, Cenedese et al., (1994) compared velocity profiles at various cross-sections in an axisymmetric free jet and an annular jet. Remarkably good agreement was obtained in the mean profiles even though only 40 PIV images were used. Disagreements were noted, however, in regions of high shear and flow reversal. Using 1800 PIV frames to evaluate the statistics in open channel flows, Nezu and Onitsuka (2001) have noted very good agreement between LDV and PIV measurements, but their comparisons were also limited to the streamwise mean velocity profiles. Nezu and Nakayama (1997) compared PIV and LDV mean velocity profiles in a compound open channel and found poor agreement near the channel junction (region of high shear) and at borders of the image analysis area. Nakagawa and Hanratty (2001) compared LDV and PIV measurements in flow over a wavy wall. Not surprisingly, comparison of Reynolds stresses using only 37 PIV images revealed near-wall discrepancies. Romano (1992) has noted larger deviations in measurements of the higher-order moments by PIV and attributed the problem to the differences in sample size, 1000 for PIV versus 20,000 for LDV. In particular, he notes that the deviations are greater in the wall-normal component. The foregoing review of previous comparisons between LDV and PIV show that they are largely limited to the primary mean velocity

component. Subsequently, PIV is employed to study flow fields, without further evaluation of data quality.

The purpose of the present paper is to describe a comprehensive and quantitative comparison of LDV and PIV measurements of mean velocity, turbulence and other quantities in a relatively complex flow that involves regions of high shear, flow reversal, and a high degree of unsteadiness. It should be noted that this assessment is limited to systems that are readily available or can be assembled by researchers who are not exclusively dedicated to development of cutting-edge techniques.

### **TEST CASE: OPEN CHANNEL FLOW OVER A BED OF FIXED DUNES**

The present study was conducted as a part of a much larger study of the physics of flow over dunes. Here, attention is given to the relative performance of LDV and PIV, and the complementary manner in which they can be used to develop a comprehensive picture of the flow.

The assessment of LDV and PIV is carried out in water flow over a train of two-dimensional dunes attached to the bottom of a laboratory open channel flume. Figure 1 shows a schematic of the flow field over a single dune of height  $h$ , wavelength  $\lambda$ , with a water depth  $d$ . Sufficiently far from entry to the flume and with the flume slope adjusted appropriately, the flow becomes periodic in space, with the flow over successive dunes being the same. Thus, it suffices to make measurements over a single dune.

The flow field contains changes in flow direction associated with separation at the dune crest and subsequent reattachment, high turbulence in the separating shear layer (Bennett and Best, 1995), presence of a free surface, and possible generation of coherent vortices in the shear layer and boils (or kolks) following reattachment (Muller and Gyr, 1987). This flow field is thus well suited to evaluate the relative performance of LDV and PIV techniques and contains much of the complexity of other practical hydraulic engineering applications.

## EXPERIMENTAL ARRANGEMENT AND PROCEDURE

The flow was generated in a rectangular cross-section (610 mm x 610 mm), 10-m long, recirculating open channel flume. A settling tank, a contraction and turbulence damping screens condition the flow at entry to the flume. The flume terminates in a diffusing section and a collection tank. A train of two-dimensional fixed dunes was attached to the bottom along the length of the channel starting near the entrance. The shape of the dunes was geometrically similar to that used in a previous study by Mierlo and Ruiter (1988). The dune height is  $h = 20$  mm, and wavelength is  $\lambda = 400$  mm, so that  $\lambda/h = 20$ , typical of many previous studies. LDV and PIV measurements were carried out in the flow over the 17<sup>th</sup> and 18<sup>th</sup> dunes, where periodicity was verified. The Reynolds number based on the dune height  $h$  and maximum velocity  $U_o$ , which occurs near the free surface,  $Re = U_o h/\nu$ , was  $1.0 \times 10^4$ . The general experimental arrangement is shown in Figure 2.

A two-component fiber-optic LDV system of standard design (TSI Inc.) powered by a 2W Ar-Ion laser was used for velocity measurements at several streamwise stations along the dune. The optical elements include a Bragg cell and a 300-mm focusing lens. The beam spacing was 50 mm and the half-angle was 3.96 deg. The system is operated in a backward scatter mode. Prior to the start of the measurements, the water in the flume was filtered with a 5  $\mu\text{m}$  filtering system, following which no measurements were possible due to the absence of scattering particles. The flow was then seeded with 5  $\mu\text{m}$   $\text{TiO}_2$  particles. The particle time constant was very low compared to the fluid time constant (based on step height and average velocity) indicating that the particles truly follow the flow (Longmire and Eaton, 1992). Following previous studies (Kang et al., 2001), tests were conducted to vary the coincidence window size and sample size to study their effects on the mean velocity, the Reynolds stresses and higher-order velocity correlations. Based on these tests, no significant differences were found in the measured variables for a coincidence window size ranging from 300 to 2000  $\mu\text{s}$ , though a decreasing data rate was noted for the more stringent window sizes. A window size of 1000  $\mu\text{s}$  was then used. Similarly, no statistically significant differences were noted by varying the sample size from 5,000 to 20,000. Data rates of the order of 60 ~ 80 Hz were

obtained while operating the system in a coincidence mode. At each measurement location, 15,000 validated samples were chosen. A standard residence time averaging procedure was used. Due to the restrictions imposed by the geometry of the transmitting optics, two-component measurements were possible only in the mid 85% of the flow depth, while one-component (streamwise velocity) measurements were made over the entire depth. Based on a 95% confidence interval, the uncertainty in the mean velocity (U and V) and turbulence intensities ( $u'$  and  $v'$ ) were estimated to be  $\pm 1.5\%$  or less. The uncertainty in the Reynolds shear stress was  $\pm 7.0\%$ . The present LDV system has been used in several studies conducted at the Institute and detailed discussions related to the usual corrections are avoided here for brevity.

For the PIV, a system of mirrors and lenses was used to generate a 3-mm thick vertical light sheet in the streamwise direction at the measuring section using a 5W Ar-Ion laser. The Plexiglas dunes facilitated the transmission of light and illumination of the flow field from the bottom of the channel. After carefully filtering the water through a 5  $\mu\text{m}$  filter, vinyl chloride polymer particles (specific gravity 1.02 and mean diameter 30  $\mu\text{m}$ ) were introduced in the flow. The Stokes settling velocity of the particles in stagnant water is negligibly small ( $< 0.2$  mm/s). These particles are therefore expected to faithfully follow the flow under the present experimental conditions. The field-of-view was imaged with CCD camera (Varifocal 5.0-40). An acousto-optic modulator (AOM) was used to enhance the dynamic range of velocity tracking (Kobayashi et al., 1991). The camera was fitted with a lens (focal-length range of 50 to 400 mm) and the object distance was adjusted to obtain a field-of-view of 120 mm in x-direction and 80 mm in y-direction. Since the dune length is  $\lambda = 400$  mm, the flow field over the dune was divided into five different fields-of-view with a 20 mm overlap between the images. Image calibration was achieved by taking a picture of a uniform square grid (10 mm x 10 mm). Using this image, the pixel size was set to 0.1876 mm/pixel (1 mm = 5.33 pixels), and the time interval between two images was set to 4 ms and the exposure time to 2.2 ms by the AOM. It was also confirmed that there was negligible image distortion over the field-of-view. A black and white frame grabber board (Data Translation DT 3155) was used to capture the images of 640 x 480 pixels and store them with 256 gray levels on a computer.

A total of 1000 frames were captured for each case with the standard frame rate of 30. The images were also simultaneously stored on videotapes.

A commercial software (Thinker's eyes 2-D) was used to perform the image analysis using a gray-level cross-correlation technique (Kimura et al., 1986, Utami and Blackwelder, 1991). Each captured frame was separated into odd and even fields to obtain the temporal information. The gray levels of the pixels in the correlation area of the first and second fields were cross-correlated within the searching area. Using an interrogation area of 20 x 20 pixels, the correlation peak was evaluated in a search area formed by a circle of radius equal to 15 pixels. Since the velocity vectors are obtained based on pixel resolution, a positional uncertainty of  $\pm 1$  pixel can occur. To enhance the accuracy, a sub-pixel resolution method (Utami and Blackwelder, 1991) was adopted. Furthermore, an error vector elimination method based on the continuous flow condition (Hojo and Takashima, 1995) was adopted. The 1000 instantaneous velocity fields were sampled to obtain the mean velocities and Reynolds stresses. The uncertainties in the mean velocities (U and V) and rms turbulence intensities ( $u'$  and  $v'$ ) were estimated to be  $\pm 2.5$  % and  $\pm 5$ %, respectively. The uncertainty in the Reynolds shear stress was estimated as approximately  $\pm 10.0$  %. Further discussion on the quality of the PIV data is provided in a forthcoming section.

## RESULTS AND DISCUSSIONS

As already noted above, surprisingly few papers in the literature show direct comparisons of LDV and PIV data beyond the mean velocity profiles. As LDV used to be validated by comparisons with hot-wire data just a few decades ago, PIV needs to be validated against the now well-established LDV as a reference. While it is generally acknowledged that conventional PIV is capable of measuring mean velocity and Reynolds stresses, it is necessary to examine the relative performance in the type of flow being considered here. Detailed information regarding the accuracy of PIV technique and error sources affecting the quality of PIV data can be found in the literature (see, for example, Adrian, 1991 and Hart, 2000). It should be remarked that the focus of the present paper is on comparison of data obtained with a conventional (easily assembled

and commercially available) PIV system with those obtained with a relatively standard LDV system, in a representative flow of practical interest in hydraulic engineering.

### Instantaneous flow field

A principal advantage of PIV is its capability to provide information about the instantaneous flow field. This is well illustrated by the two sets of successive instantaneous images shown in Figure 3. They correspond to two overlapping fields-of-view, taken at different times. In the region of the dune crest (Figure 3a), at time  $t = t_0$ , there appear to be two vortical structures, one just forming below the shear layer emanating from flow separation at the crest, and the other farther downstream. The former is small and nascent while the latter is larger and more diffused. With increasing time, the latter moves out of the field-of-view while the former grows in size and travels downstream at a velocity of about  $0.4U_0$ . In the last frame, this vortex is seen to again decrease in size. The subsequent evolution of this vortex could not be tracked due to limitation of the field-of-view – a limitation that is set by the PIV configuration and available instrumentation. The second sequence of images (Figure 3b) shows the organized motions in a region downstream of the first. Here, the presence of strong ejection and sweep-type events that can have important implications in the transport of sediments as well as other types of event have been observed; including the generation of larger-scale vortical (organized) structure developed farther downstream and active interactions with slowly varying main stream, rather weak formation of organized structure depending on time sequence, and so on.

It is important to recognize that the relatively inexpensive and simple PIV system employed here provides information that cannot be obtained by LDV. Further processing of the PIV images using some of the techniques suggested by Adrian et al. (2000) could provide more quantitative information, such as the length and time scales of the observed flow structures.

### Time-averaged flow field

Figure 4 shows typical time-averaged results in a viewing window 120 mm long and 80 mm high. Averaging is done over 1000 PIV images. In contrast to Figure 3,

Figure 4a shows well-defined mean streamlines and a zone of reverse flow. Determination of the point of reattachment by visual inspection is misleading, however. Analysis of the near-wall LDV data indicate that the mean reattachment point is at  $X/h = 4.5$  ( $X/\lambda = 0.225$ ). Figure 4b shows contours of the spanwise component of mean vorticity calculated by simple central differences in the measured velocity components. It is seen that the shear layer arising from separation at the dune crest is well identified by the zone of high vorticity. Comparison with the instantaneous flow in Figure 3a shows that time averaging hides much of the wavy and unsteady structure of the actual shear layer. Figure 4c shows contours of the Reynolds shear stress ( $\overline{u'v'}$ ) calculated by subtracting the mean values of the velocity components from their instantaneous and then averaging their product over the 1000 data sets. The shear layer is evident from the regions of high turbulent shear stress. This is also the region of largest turbulence intensities (not shown).

Figure 5 shows the profiles of the x-component of mean velocity ( $U$ ), the rms turbulence intensities in the x- and y-directions ( $\sqrt{u'^2}, \sqrt{v'^2}$ ), and the Reynolds shear stress ( $-\overline{u'v'}$ ) at three representative streamwise stations, namely,  $X/h = 5, 12$  and  $-2$  (same as  $X/h = 18$  due to space periodicity). All the variables are made dimensionless by the maximum velocity  $U_o$ , held constant at 0.48 m/s in the experiments. The dune height ( $h$ ) is used as the normalizing length scale at each station. The corresponding values of  $X/\lambda$  are noted on the figures. These figures provide a direct comparison between PIV and LDV data. The first station (Figure 5a) is located just downstream of the mean reattachment point which, as noted above, was determined from near-wall LDV data to be at  $X/h = 4.5$ , the second and third are in the region of flow recovery and gradual acceleration, the third station being just ahead of the dune crest.

The limitation of the PIV field-of-view (and quality of light sheet) is clear from the limited extent of the data in the vertical direction. Also seen is the limitation of the two-component LDV in the near-wall region due to blockage of the beams by the dune. These limitations of the two systems are obvious, and present in most arrangements although their criticality will depend on the flow, or flow region of interest. In general, the PIV and LDV data show agreement within the expected uncertainties of the two

systems in the mean velocity and turbulence intensities. The agreement in the shear stress is good at the first station in spite of the high shear and intermittent flow reversal (see Figure 3) but PIV gives larger values of the shear stress at the two downstream stations. The reason for this is not known although the rather poor illumination of light sheet at these locations may have deteriorated the image quality.

Figure 5 also shows that both LDV and PIV are capable of measuring traditional mean-flow and turbulence quantities even in regions of flow separation and high shear, and providing quantitative information about major flow features. For example, the peak in the  $u'$  profiles at  $y/h \sim 1.0$  is due to the shear layer emanating from the dune crest, while the much smaller peak farther from the bed ( $y/h \sim 2.5$ ) is the remnant of the turbulence carried over from the shear layer shed of the previous dune. In general, the PIV data is far better than would be expected from this rather simple and conventional system. It is worth mentioning here some key parameters employed for PIV data reduction to obtain the mean velocity and turbulence quantities. Almost always good results were obtained for mean velocity profiles over entire flow field, regardless of interrogation area and searching distance, and even image-processing technique. Results were also less sensitive to the quality of the image, such as brightness, contrast, etc. The converged mean values were obtained with as few as 200 images. The turbulence quantities, on the other hand, were much more sensitive to the size of the interrogation area as well as searching distance. Results were affected considerably by an error removing process as well as by the quality of the image. As many as 1000 images were required to obtain converged results, and this number greatly depends on the size of interrogation area. While it is obvious that the interrogation area should be small enough to resolve the size of eddies involved in the flow, a larger interrogation area provides more stable (converged) results even with a smaller number of frames.

#### Time series data and two-point correlation

Successive instantaneous PIV images may be converted into time series of data at different points in space to obtain further quantitative information, such as space- and auto-correlations, and frequency of events with quadrant analysis. Figure 6 shows the time series of the two velocity components at two typical locations. The first ( $X/h = 4$ ,

$Y/h = 2.1$ ) is outside the mean re-circulation region and shows smaller fluctuations. The second point ( $X/h = 4$ ,  $Y/h = 0.7$ ) is close to the mean separation streamline where the velocity gradients and turbulence are high. Only a fraction of the 1000 data points obtained with a time interval of  $(1/30)$  s is shown in each case.

One of the benefits of PIV is the capability to obtain spatial correlations, such as the two-point space correlation  $C_{u_i u_j}$  :

$$C_{u_i u_j} (x_o, y_o ; dx, dy) = \frac{\overline{u_i' (x_o, y_o, t) u_j' (x_o + dx, y_o + dy, t)}}{\sqrt{\overline{u_i'^2} (x_o, y_o)} \sqrt{\overline{u_j'^2} (x_o, y_o)}}$$

where,  $i = 1$  or  $2$ ,  $j = 1$  or  $2$ ;  $u_1 = u$ ,  $u_2 = v$ , and  $\sqrt{\overline{u_i'^2}}$  is the standard deviation of  $u_i$ . Nezu and Nakayama (1997) have suggested that such correlations are useful to analyze general properties of large-scale coherent vortices generated in open-channel flows. Figure 7 shows, the correlation coefficients  $C_{uu}$  and  $C_{vv}$  calculated using all 1000 images at  $X/h = 4.0$ ,  $Y/h = 0.53$ , on the mean separation streamline near the mean reattachment point. In the present case,  $C_{uu}$  shows much higher streamwise correlation, indicating a larger turbulence length scale in x-direction. Further analysis of these correlations provides various length scales of turbulence, as noted by Nakagawa and Hanratty (2001).

#### Quadrant analysis

A quadrant analysis was carried out using the method of Lu and Willmarth (1973). To detect extreme events (making large contributions to the turbulent shear stress), a detector indicator function  $\lambda_i(t)$  was defined such that:

$$\lambda_i(t) = \begin{cases} 1 & \text{when } |u'v'|_i \geq H(u')(v') \\ 0 & \text{otherwise} \end{cases}$$

where,  $i$  denotes the quadrant of interest. The contribution to  $\langle u'v' \rangle$  from a particular quadrant may then be written:

$$\langle u'v' \rangle_i = \lim_{T \rightarrow \infty} \frac{1}{T} \int_0^T u'v' \lambda_i(t) dt$$

Here, results are presented for  $H = 2.0$ , which corresponds to events which are associated with  $(u')(v') > 5.5 \langle u'v' \rangle$ . Since 1000 data points, corresponding to the 1000 PIV images, turned out to be insufficient for such conditional sampling of extreme events, data at two adjacent axial locations were utilized at each location. Therefore, total of 3000 data points were used for the calculations at each location, compared to the 15,000 data for LDV.

Fractional contribution by each one of the quadrants is shown in Figure 8 for  $X/h = 4$ . Even at this level of analysis, the results of LDV and PIV are in close agreement. It is seen that PIV provides information in the near-wall region ( $y/h < 1$ ) while LDV provides information for  $y/h > 3$  due to the limitations of the two systems discussed above. The quadrant-two events (ejections) make a larger contribution to the shear stress through most of the depth and indicate a peak in the region of the shear layer. The second peak in the quadrant-four (sweep events) profile occurs at a wall normal location that corresponds to a local minimum in the ejection event.

## **FURTHER DISCUSSION ON THE ACCURACY OF PIV**

### Interrogation area and searching distance

Accuracy and quality of velocity vectors obtained with PIV are usually greatly affected by the choice of the interrogation area and the searching distance. The number of grid points where the velocity vector is calculated is also very important to enhance the spatial resolution, but it is inherently limited by the size of the interrogation area. Keeping the interrogation area as small as possible is crucial, but that is a difficult task since it requires at least one or two seed particles in each interrogation area. Also, determination of the smallest turbulent eddy to be resolved is difficult to do ahead of the

experiment. In the present case, a grid size of 3 x 2 mm in the (x, y) directions was chosen, with the interrogation area and the searching distance approximately 3.5 x 3.5 mm<sup>2</sup> and 5~6 mm, respectively, depending on the local flow velocity. Good agreement of the Reynolds stresses with the LDV data shown in Figure 5 implies that contributions from the relatively large-scale turbulent flow structures with low frequency (slowly moving eddies) made up most of the Reynolds stress. In other words, motions at scales smaller than 3.5 mm had a negligible effect on the magnitude of the Reynolds stress.

Choice of the interrogation area and the searching distance depends on the relative length scale of the experimental model. For example, the flow of Nakagawa and Hanratty (2001) is very different from the present one. The length and height of their wavy wall were 5 and 0.25 mm, respectively, and their interrogation area was 1.4 x 1.3 mm<sup>2</sup>. In the present experiments, the dune length and height are 400 and 20 mm, respectively, and the interrogation area is 3.5 x 3.5 mm. Thus, in a given application, the turbulence length scale should determine the interrogation area.

#### Effect of time resolution

The time series data of Figure 6 show a typical turbulent flow signal. It should be noted that 1000 data points and time resolution of (1/30)s may be insufficient to satisfactorily perform spectral analysis. However, it is known that coarse time resolution does not limit the accuracy of Reynolds-averaged values (mean velocity, turbulence, etc.) and may even be advantageous because it provides more uncorrelated time series data and thereby accelerates convergence. Time resolution does not have any effect on quadrant analysis either because in quadrant analysis there is no process requiring precise information on small scale eddies. However, time resolution becomes very important to study turbulent dissipation processes or energy transfer from the larger to the smaller eddies.

#### Effect of total number of data

While the sample size in PIV may not be a problem in obtaining time-averaged mean velocity and vorticity, it can be a major shortcoming in measurement of turbulence quantities and higher-order correlations. In the present case, approximately 200 frames

were found to be enough to measure the mean velocities at most locations, but at least 500 frames were necessary for Reynolds-averaged turbulence quantities to achieve moderate degrees of accuracy, with 1000 frames giving better accuracy.

The size of one raw-formatted image captured by a conventional 640 x 480 image grabber is usually a little larger than 300 KB. So, 300 MB are required to gather 1000 sets of data for one field-of-view. Processing time and disk storage are also a problem. It usually takes one day on a Pentium III Desktop PC to process 1000 frames, although the processing time greatly depends on the size of the interrogation area as well as searching distance. In the present experiment, where images from five 120 x 80 mm fields-of-view were combined to construct the whole field on a single dune, a 1.5 GB disk storage and 5 days of processing time were required. This would expand to 5 GB and 17 days if a 1K x 1K camera or image grabber is to be employed! This shows the large amounts of memory size that would be needed to extract conditionally sampled or phase-averaged information from PIV data.

#### Particle size and density

It is well known that more particles yield better correlations in PIV, unless the water is too contaminated by particles or there is blockage of light by the particles. Other considerations also enter the selection of particle size. A 30-micron diameter particle used here is quite large, and may not be adequate for measurements seeking to accurately resolve small-scale turbulence. It is however very good for brighter and clear particle images, which are crucial for a camera and image grabber with modest level of resolution (640 x 480), as employed in the present study. Considering the quality of data presented above, it is concluded that relatively large particle size may be good enough for many practical hydraulic and hydrodynamic experiments, including the measurement of turbulence. In general, however, selection of particle size depends on the details of the PIV system.

There are other factors affecting the quality of the PIV image. For example, the depth of field due to the thickness of the laser light sheet can induce errors in highly three-dimensional flow, because part of the out-of-plane velocity component may be included in the in-plane components depending on the viewing angle. Ambiguity of the

flow field near the air-water interface also needs to be considered for open-channel flow applications.

## **CONCLUSIONS**

A relative assessment of LDV and PIV techniques is made in a complex turbulent flow typical of those encountered in practical hydraulic engineering. The LDV and PIV systems used here may be readily purchased or assembled without a great deal of expense. It is shown that even a modest PIV system, with commercially available software, yields mean velocity and turbulence data even in regions of high shear, turbulence and flow reversals. In addition, the instantaneous flow fields recorded by PIV provide quantitative information about coherent structures that is not readily measured by LDV. It is shown that PIV may be used to measure two-point correlations and make quadrant analysis with accuracy comparable to LDV. As this paper is concerned with comparison between LDV and PIV data, further discussion of the physics of flow over a dune is deferred to a separate paper (Balachandar et al., 2003).

## **ACKNOWLEDGMENTS**

This study was conducted during a period when the first two authors spent their sabbatical leaves at IIHR. The authors acknowledge the cooperation of Dr. Marian Muste in accommodating this study in the experimental facilities used in his research program, and his assistance in keeping the equipment operational over the course of the experiments. Darian Dejong, Doug Houser and Mark Wilson of IIHR staff provided invaluable help in the planning and conduct of the experiments.

## **REFERENCES**

- Adrian, R.J., 1997, Dynamic ranges of velocity and spatial resolution of particle image velocimetry, *Meas. Sci. Technol.* Vol. 8, pp. 1393-1398.
- Adrian, R.J., 1996, Bibliography of particle velocimetry using imaging methods: 1917-1995, Technical Report 817, University of Illinois.

Adrian, R.J., 1991, Particle imaging techniques for experimental fluid mechanics, Annual Rev. Fluid Mechanics, Vol. 23, pp. 261-305.

Adrian, R.J., Christensen, K.T. and Liu, Z-C., 2000, Analysis and interpretation of instantaneous turbulent velocity fields, Experiments in Fluids, Vol. 29, pp. 275-290.

Balachadar, R., Hyun, B-S., Polatel. C. and Patel, V. C., 2002, The structure of flow over a fixed dune: Effect of depth, Under Submitted to the J. Hydraulic Engineering, ASCE.

Bennett, S. J. and Best, J. L., 1995, Mean flow and turbulence structure over a fixed bed, two-dimensional dunes: implications for sediment transport and bedform stability, Sedimentology, Vol. 42, pp. 491-513.

Cenedese, A., Doglia, G. and Romano, G.P., 1994, LDV and PIV velocity measurements in free jets, Experimental Thermal and Fluid Science, Vol. 9, pp. 125-134.

Goldstein, R.J., 1996, Fluid Mechanics Measurements, 2<sup>nd</sup> Edition, Taylor and Francis, London, U.K.

Hart, D.P., 2000, PIV error correction, Experiments in Fluids, Vol. 29, pp. 13-22.

Hojo K. and Takashima H., 1995, Detection of erroneous velocity vectors obtained in PIV, J. Visualization Society of Japan, Vol.15, Suppl. No.2, p. 177.

Kang, S., Patil, B. and Roy, R.P., 2001, Effects of coincidence window and measuring volume size on laser Doppler velocimetry measurement of turbulence, Experiments in Fluids, Vol. 30, pp. 365-370.

Keirsbulck, L. Labraga, L., Mazouz, A. and Tournier, C., 2002, Surface roughness effects on turbulent boundary layer structures, J. Fluids Engineering, Vol. 124, pp. 127-135.

Kimura I., Takamori T. and Inoue T., 1986, Image processing instrumentation of flow by using correlation technique, Flow Visualization, Vol.6, No.22, p. 105.

Kobayashi, T., Saga, T., Haeno, T. and Tsuda, N., 1991, Development of a real-time velocimetry measurement system for high Reynolds fluid flow using a digital image processing design, ASME FED-Vol.128, pp.1220-1227.

Longmire, E.K., and Eaton, J.K., 1992, Structure of a particle-laden round jet, J. Fluid Mechanics, Vo. 236, pp. 217-257.

Mierlo, M.C.L.M. and de Ruiter, J.C.C., Turbulence measurements above artificial dunes, Rept. Q789, Delft Hydr. Lab., Delft, The Netherlands.

Muller, A. and Gyr, A., 1986, On the vortex formation in the mixing layer behind dunes, J. Hydraulic Research, IAHR, Vol. 24, No. 5, pp. 359-375

Nakagawa, S. and Hanratty, T.J., 2001, Particle image velocimetry measurements of flow over a wavy wall, *Physics of Fluids*, Vol. 13, No. 11, pp. 3504 – 3507.

Nezu, I., Kadota, A., Shinbashi, H. and Kuata, M., 1997, Conditional sampling analysis on coherent vortices in unsteady open-channel flows over dune bed, *Proc. Environmental and Coastal Hydraulics: Protecting the Aquatic Habitat*, Vol. 2, 27<sup>th</sup> Congress of IAHR, San Francisco, pp. 1209-1214.

Nezu, I. and Nakayama, T., 1997, Space-time correlation structures of horizontal coherent vortices in compound channel flows by using particle-tracking velocimetry, *J. Hydraulic Research, IAHR*, Vol. 35, No. 5, pp. 191- 208.

Nezu, I. and Onitsuka, K., 2001, Turbulent structures in partly vegetated open-channel flows with LDV and PIV measurements, *J. Hydraulic Research, IAHR*, Vol. 39, No. 6, pp. 629-642.

Raffel, M., Willert, C. and Kompenhans, J., 1998, *Particle Image Velocimetry: a Practical Guide*, Heidelberg, Springer.

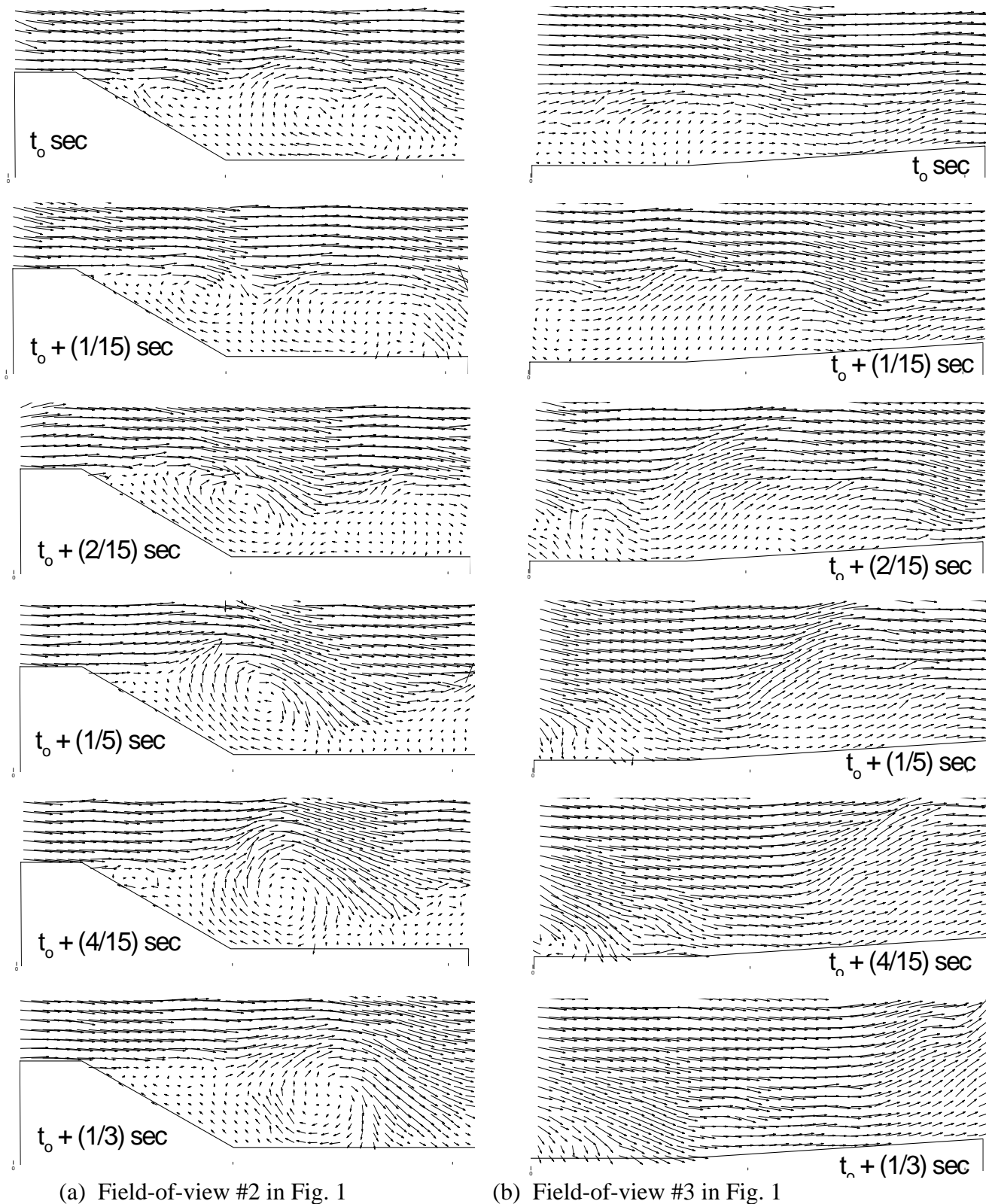
Romano, G. P., 1992, PIV and LDV velocity measurements near walls and in the wake of a delta wing, *Optics and Lasers in Engineering*, Vol. 16, pp. 293-309.

Shineeb, A., Bugg, J. D. and Balachandar, R., 2002, PIV measurements in a confined jet, Paper No. FEDSM2002-31160, ASME, Fluids Engineering Division Summer Meeting, Montreal, Canada.

Utami T. and Blackwelder R., 1991, A cross correlation technique for velocity field extraction from particulate visualization, *Exp. in Fluids*, Vol.10, pp.213-223.

Yeh, H. and Cummins, H. Z., 1964, Localized fluid measurements with a He-Ne laser spectrometer, *Appl. Phys. Lett.* Vol. 4, 176-178.

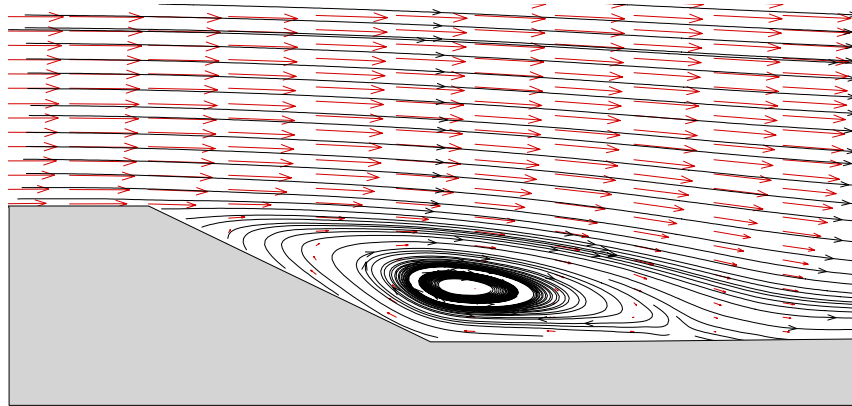




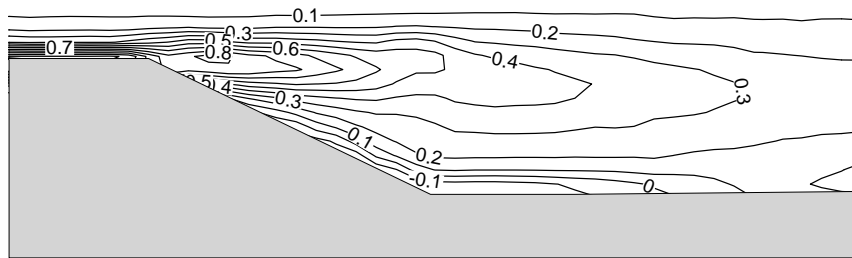
(a) Field-of-view #2 in Fig. 1

(b) Field-of-view #3 in Fig. 1

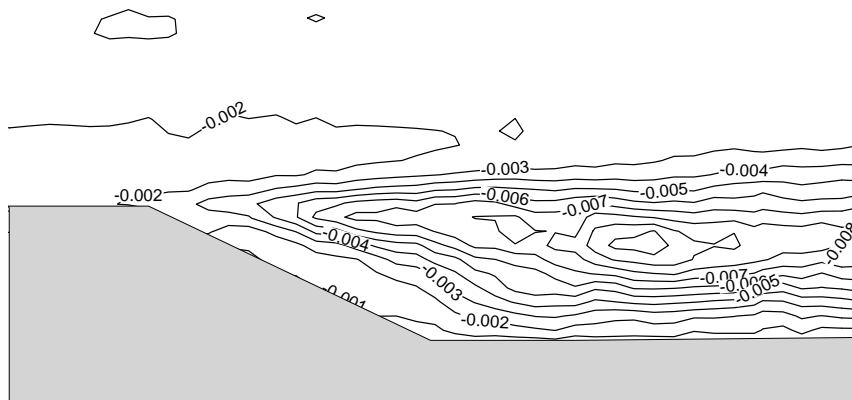
Fig. 3. Instantaneous velocity field obtained by PIV



(a) Velocity vectors and streamlines

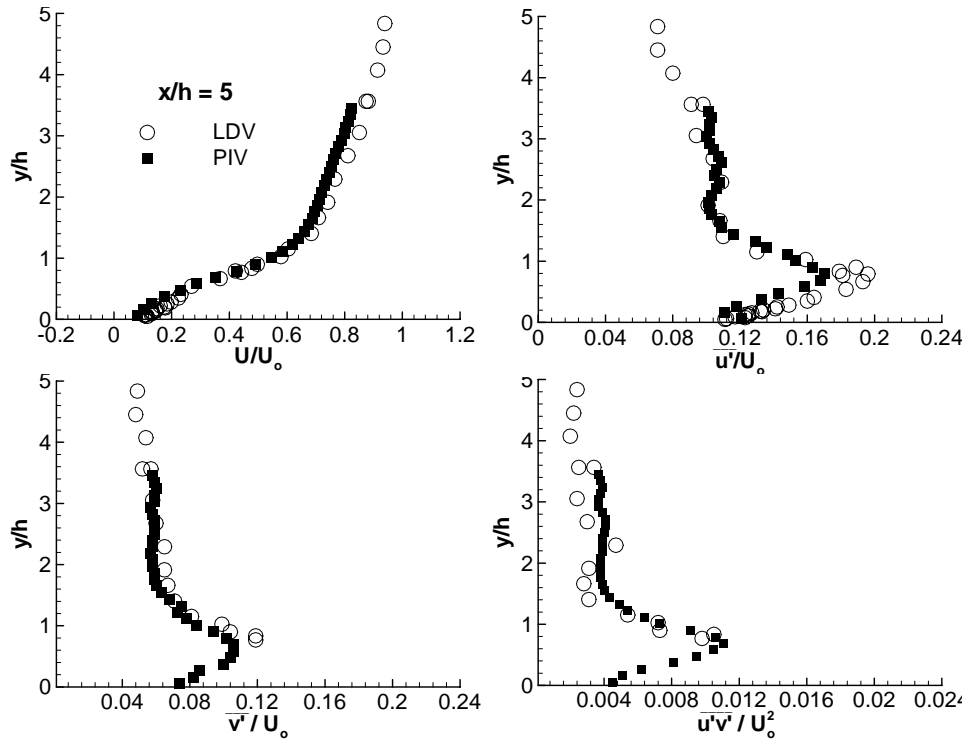


(b) Vorticity field

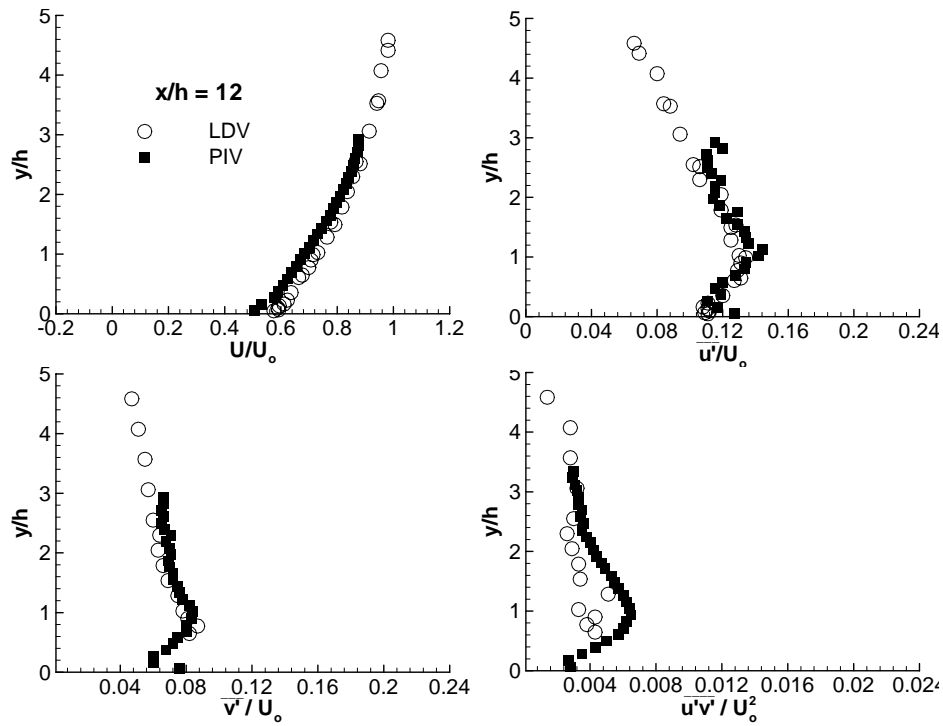


(c) Shear stress  $\overline{u'v'}$

Fig. 4. Time-averaged flow field by PIV

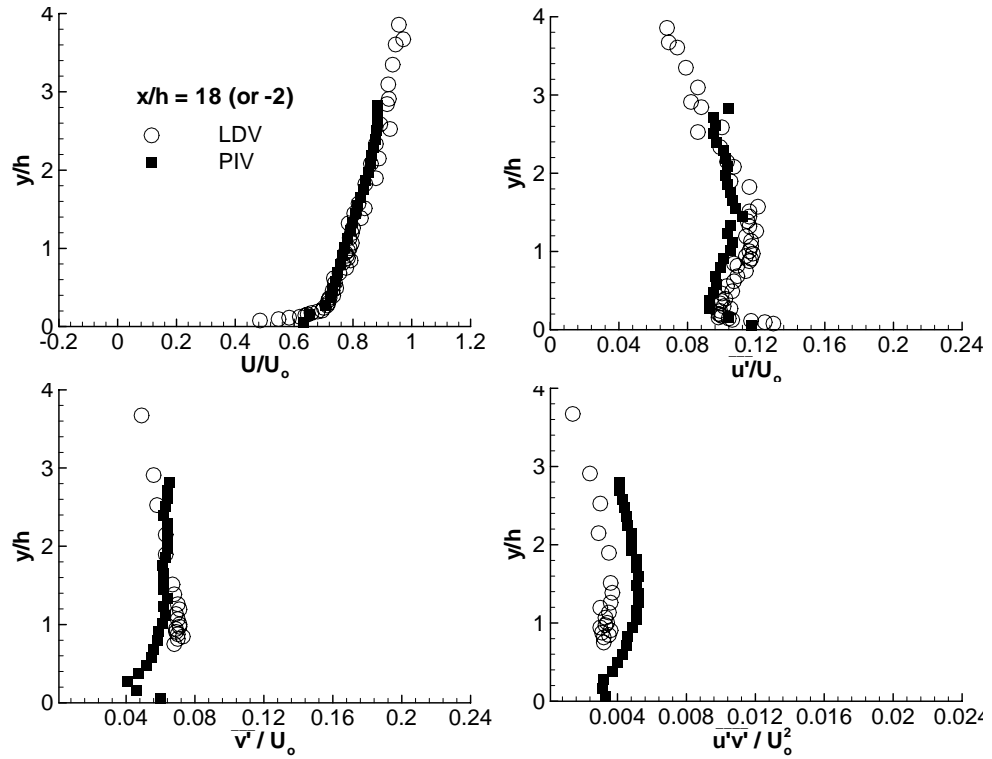


(a)  $X/h = 5, X/\lambda = 0.25$



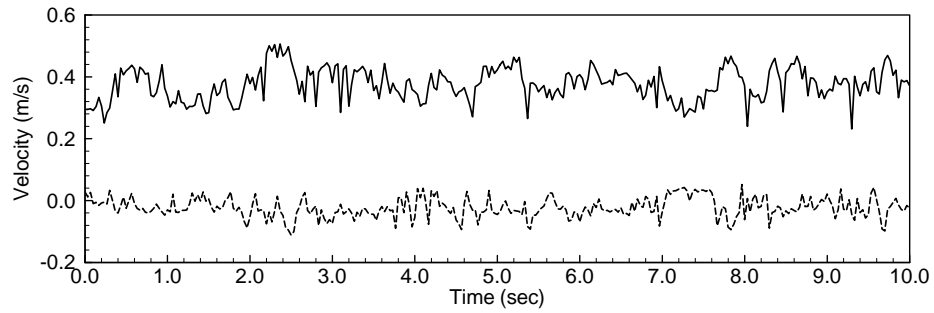
(b)  $X/h = 12, X/\lambda = 0.6$

Fig. 5. Comparison between PIV and LDV data

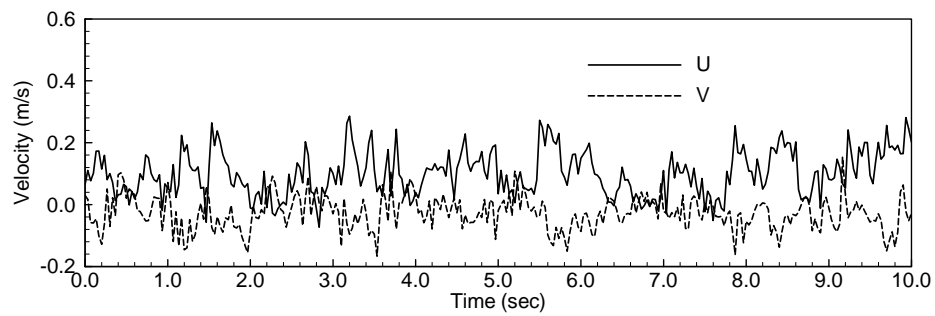


(c)  $X/h = -2$  (same as 18),  $X/\lambda = 0.9$

Fig. 5. (Continued)



(a)  $y/h = 2.1$



(c)  $y/h = 0.7$

Fig. 6. Time series data from PIV

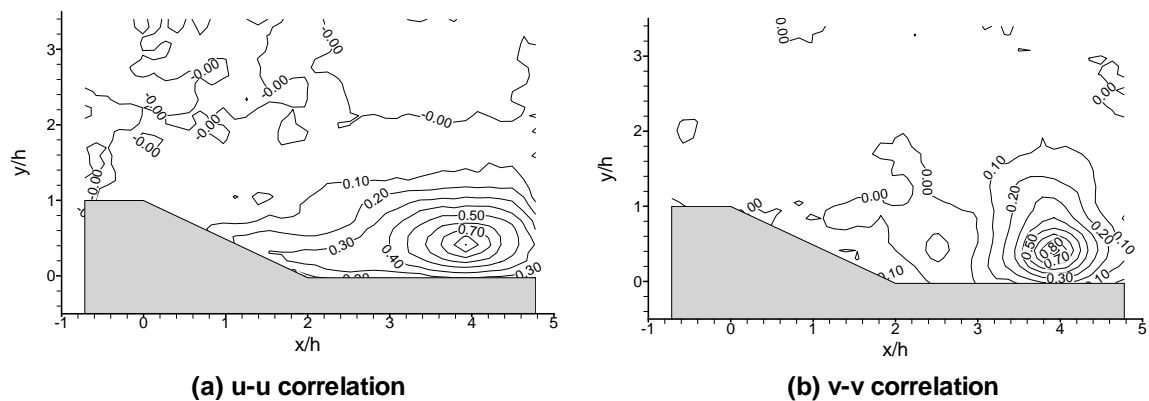


Fig. 7. Two-point correlations at  $X/h = 4$ ,  $Y/h=0.53$

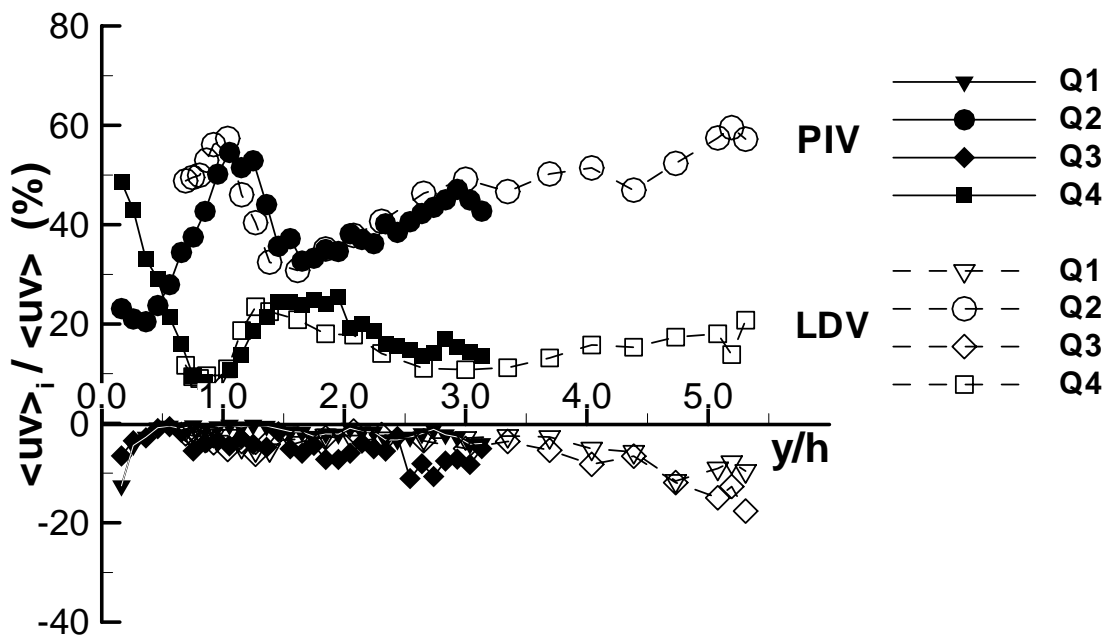


Fig. 8. Quadrant analysis at  $X/h=4$ ,  $X/\lambda = 0.2$